Nuclear Instruments and Methods in Physics Research B 267 (2009) 2987–2990

Contents lists available at ScienceDirect

Nuclear Instruments and Methods in Physics Research B

journal homepage: www.elsevier.com/locate/nimb

Assessment of approximations for efficient topography simulation of ion beam processes: 10 keV Ar on Si

Christoph Ebm [a], Gerhard Hobler [b,*]

[a] IMS, Nanofabrication AG, Schreygasse 3, A-1020 Vienna, Austria
[b] Institute of Solid State Electronics, Vienna University of Technology, Floragasse 7, A-1040 Vienna, Austria

ARTICLE INFO

Article history:
Available online 14 June 2009

PACS:
68.49Sf
79.20Ap
79.20Rf
81.16Nd
81.16Rf

Keywords:
Focused ion beam
Multi ion beam-system
Ion milling
Sputtering
Gas-assisted deposition
Binary collision simulation
Topography simulation

ABSTRACT

The main assumption of existing efficient topography simulations is that sputtering is a local process that depends only on the angle of incidence and not on the detailed shape of the surface. If redeposition is considered, sputtered atoms are redeposited and cause no further sputtering when they hit another part of the surface. Furthermore the angular distribution of sputtered atoms follows a cosine law. If ion reflection is considered, ions do not lose energy during backscattering. Using binary collision simulations (IMSIL) and comparing them with results obtained by a topography simulator (IonShaper®) we show that all these assumptions need refinement for the simulation of nanostructures except the neglect of sputtering by sputtered atoms. In addition we show that a nonlocal model is essential for ion beam induced deposition of narrow structures.

1. Introduction

Ion beams are versatile and increasingly used tools for the fabrication of nanostructures either by direct milling [1] or by gas assisted processes [2]. The present study is motivated by efforts to fabricate stamps for nanoimprint lithography with a massive multi ion beam-system [3–6]. In all applications simulation can help to understand the physical processes and to optimize the shape of the structures.

Most existing codes for computationally efficient topography simulation of ion beam processes [7–16] track surface propagation explicitly, following the history of surface points thought to be connected by straight segments. All codes are based on the assumption that the sputtering yield is a function of the angle between the incident ion and the local surface normal. This usually is a good approximation for structures in the micrometer range but becomes increasingly questionable when typical feature sizes are on the order of the ion projected range or below. Only some codes include redeposition [8,10,14–16] and only a few secondary sputtering by backscattered (reflected) ions [14]. These effects are particularly relevant in high aspect ratio structures like deep trenches. Fig. 1 shows the contours of trenches sputtered by a 200 nm wide homogeneous ion beam at two different times, calculated with the IonShaper® software [14]. At either time simulations without redeposition and reflection (dash-dotted lines) are compared with simulations considering redeposition only (dashed lines) and considering both redeposition and reflection (solid lines). It can be seen that redeposition of atoms sputtered from the trench bottom leads to a narrowing of the trench towards the bottom. At a later stage (not shown), redeposition from the sidewalls to the bottom and to the other sidewall leads to a decrease of the overall milling efficiency [14,15]. Reflection of ions from the sidewalls leads to the formation of microtrenches at the trench bottom near the sidewalls. Moreover, the increased sputtering yield at the now inclined surface of the microtrenches leads to additional redeposition at the sidewall.

In calculating the redeposition flux, a cosine law [17] is used to describe the angular distribution of the sputtered atoms. Ion backscattering is assumed to be without energy loss. Furthermore, sputtered atoms that reach another point on the surface are redeposited there and cause no further sputtering. These assumptions as well as the local approximation of sputtering are investigated in this paper using binary collision simulations. We restrict ourselves to 10 keV Ar ions and Si targets which is our current focus of interest.

* Corresponding author. Tel.: +43 1 58801 36233; fax: +43 1 58801 36291.
E-mail address: gerhard.hobler@tuwien.ac.at (G. Hobler).

0168-583X/$ - see front matter © 2009 Elsevier B.V. All rights reserved.
doi:10.1016/j.nimb.2009.06.014

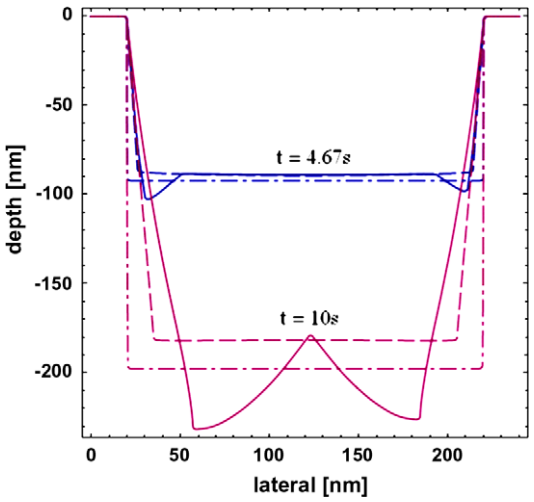

Fig. 1. Trenches sputtered by a 200 nm wide 10 keV Ar beam with a current density of 10 mA/cm^2 after 4.67 and 10 s. Dash-dotted lines: no redeposition and no ion reflection, dashed line: redeposition but no ion reflection, solid line: with redeposition and ion reflection.

2. Simulation

2.1. Topography simulation

Two-dimensional (2D) topography simulations are performed with the IonShaper® software [14]. In short, the surface is described by a sufficient number of points which are moved perpendicular to the average slope of the adjacent line segments. The velocities of the points are calculated from the fluxes of atoms sputtered by the incident ion beam and by ions reflected from other parts of the surface, and from the fluxes of redeposited atoms originating from sputtering at other surface points [14]. Sputtering is treated as a local process, i.e. the flux of sputtered particles at a certain surface point depends only on the flux of incident ions at that point and their angle with respect to the surface normal.

In reality, because of the finite range of the recoils, the sputtered atoms are ejected from an area around the incidence point. This may play an important role in case of nonplanar surfaces. In order to investigate this effect, we have additionally implemented a nonlocal model for the sputtering flux. The amount of recoils at a given surface point (destination point) resulting from the impingement of ions at another surface point (source point) is calculated from the distance between the two points and the angle between the line connecting the points and the ion incidence direction. For this purpose tables are used that have been obtained by binary collision simulations of the recoils reaching the surface for various incidence angles at a planar surface. As an option, for a concave shape of the surface between source and destination point, the distance between the points can be replaced by the distance along the surface in the table look-up.

The original version of IonShaper® contained a model of beam induced deposition which included precursor coverage calculation and a simple implementation of the nonlocal effect of the ions on the deposition rate [14]. It has been shown that the deposition rate is proportional to the number of recoils reaching the surface [18]. Therefore we have improved the deposition model using the recoils based model described above.

2.2. Binary collision simulations

Binary collision simulations are done with the IMSIL code [19]. IMSIL has been used for ion implantation studies in one- and two-dimensional targets. In this work we only use amorphous targets, since Si easily amorphizes upon ion bombardment. IMSIL has been enhanced for sputtering calculations in two respects. First, the planar model of the surface potential [20] has been implemented. While this is straightforward in 1D targets, it is more involved in the case of surfaces given by polygons in the 2D case because of the need to follow trajectories to some distance outside the target and to calculate the surface normal there. We do this by covering the simulation area with a fine grid and calculating the signed distance of each node from the surface. During the simulation of a recoil trajectory, the distance of the recoil from the surface is calculated by interpolation in the tabulated values. If the distance of a new recoil position from the surface exceeds the maximum impact parameter p_{max} the recoil is put back to the point of the preceding free flight path that is at a distance p_{max} from the surface. The surface normal at this point is calculated by the gradient of the distance function. In general, recoils leaving the surface are checked for entering the target somewhere else. For the purpose of this study, however, the recoils are stopped when they leave the target. An effective surface binding energy of 4.1 eV has been determined by fitting experimental sputtering yields [21].

Second, special care must be taken to treat glancing incidence correctly. In order to avoid unrealistic close encounters when entering the target, the ions must start at a distance p_{max} from the surface. Collisions are only executed if the hit target atom actually is inside the target. Moreover, very small mean free flight paths are used for the ion outside the target. However, even then the results may depend on assumptions about the free flight paths. This is because the distribution of free flight paths implicitly determines the roughness of the surface. We therefore use a Poisson distribution for the free flight paths which provides a well-defined model of the target. Together with the rejection of collision partners outside the target it guarantees constant atom density inside and zero density outside the target.

3. Results

3.1. Angular distributions

Fig. 2 shows the angular distributions of sputtered and backscattered atoms obtained by binary collision simulations for incidence angles of 0°, 40°, 70° and 87°. With increasing incidence angle the distributions increasingly deviate from the cosine rule (indicated by the sphere). The deviation is significant in particular

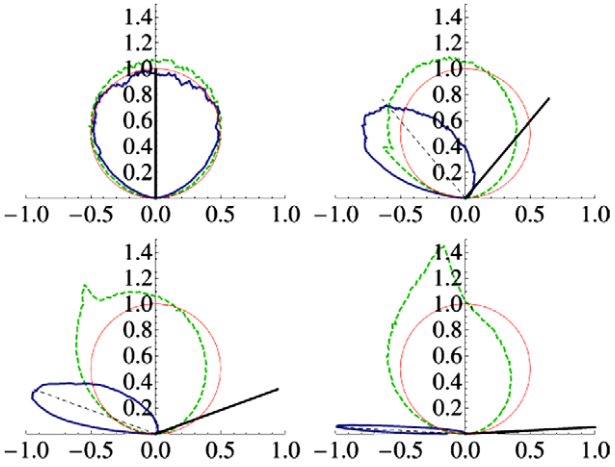

Fig. 2. Angular distribution of sputtered atoms (dashed) and reflected ions (solid) compared to a cosine distribution (circle) for incidence angles of 0°, 40°, 70° and 87°.

for milling of deep trenches, since the fluxes in backward direction (to the right in Fig. 2) determine how many atoms may leave the trench.

The angular distribution of backscattered ions can only roughly be described by specular reflection (straight dashed lines). The distribution is more shifted towards exit angles perpendicular to the surface with larger standard deviations at smaller incidence angles. The angular distribution of the reflected ions determines the shape of the microtrenches shown in Fig. 1 and should therefore be described accurately.

3.2. Secondary sputtering

IonShaper® assumes that redeposited atoms do not sputter and that reflected ions sputter with the same yield as the incident ions. To quantify the validity of this assumption we have calculated average sputtering yields of sputtered atoms and backscattered ions for normal incidence (Y_{ss} and Y_{sb}, respectively) taking into account the energy distribution of the sputtered atoms/backscattered ions determined from the binary collision simulations. The energy dependence of the normal-incidence sputtering yield is described by an analytical formula [22]. Since in the case of Y_{ss} we are interested only in a rough estimate, we approximate the yield of the sputtered Si atoms by the sputtering yield of Ar ions.

Fig. 3 shows the secondary sputtering yields Y_{ss} and Y_{sb}. For very grazing incidence Y_{sb} is close to the sputtering yield of the incident ions ($Y_s = 1.47$ [22]), but it decreases significantly when the angle of incidence is reduced (e.g. by ~30% at 80°; note that sidewall angles in Fig. 1 are between 77° and 86°). In contrast, the average sputtering yield Y_{ss} of sputtered atoms is rather small and probably negligible in most cases.

3.3. Nonlocal effects

In order to investigate nonlocal effects, we have taken the contour of Fig. 1 at 4.67 s and calculated the primary sputtering flux according to various models. The results obtained with the local model are shown by the dash-dotted line in Fig. 4, while the binary collision results are depicted with the solid line. Several remarkable differences can be seen. Immediately right to the lateral coordinate of 20 nm and left to 50 nm the local results overestimate the flux. In the first case this is because the beam is limited to >20 nm, and the contribution of recoil cascades of ions impinging at <20 nm

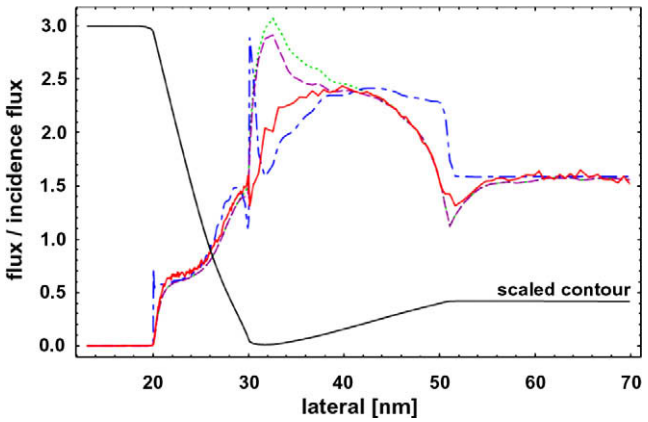

Fig. 4. Primary sputtering flux along the surface using various models: solid line: obtained from binary collision simulations, dash-dotted line: local model, dotted line: model considering the recoil range, dashed line: model using the surface length instead of the distance between source and destination point in the recoil range model. The displayed contour is scaled to fit the plot area, so angles appear smaller.

is missing in the binary collision results while it is erroneously taken into account in the local model. At 50 nm there is an incoming flux at >50 nm, but the incidence points are deeper than if the contour were extended to >50 nm with the slope at <50 nm. It is therefore harder for the recoils originating from ions at >50 nm to get back to the surface at <50 nm. This is reflected by the binary collision results, but not by local model. At ~30 nm two sharp peaks are seen in the local model which are due to the change in slope first towards larger values (negative peak) and then towards lower values passing to the yield maximum (positive peak). These changes in slope are so rapid that they are not seen in the binary collision results due to the smearing effect of the finite size of the recoil cascade.

The dotted line corresponds to IonShaper® results obtained with the table-based recoil model described in conjunction with the deposition model. It can be seen that they follow the binary collision results over the most part. Only at the bottom of the microtrench (>30 nm) a peak can be observed that is not present in the binary collision results. It is due to the fact that at a concave surface the path from the ion incidence point to the destination

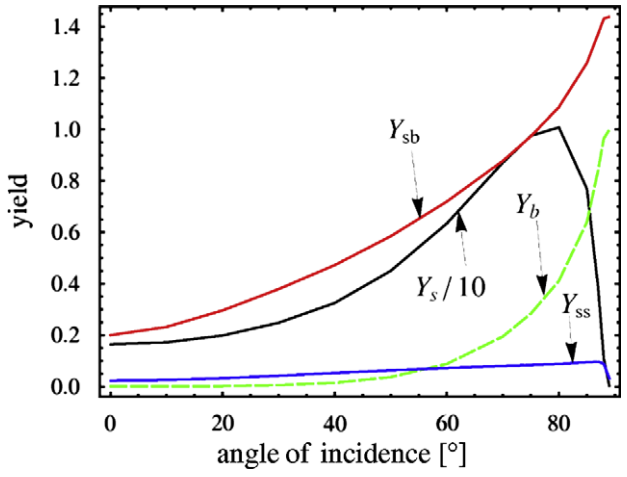

Fig. 3. Primary and secondary yields as a function of primary ion incidence angle as calculated by binary collision simulations. Primary sputtering yield Y_s, backscattering yield Y_b, average sputtering yield of sputtered atoms at normal incidence Y_{ss} and average sputtering yield of backscattered ions at normal incidence Y_{sb}.

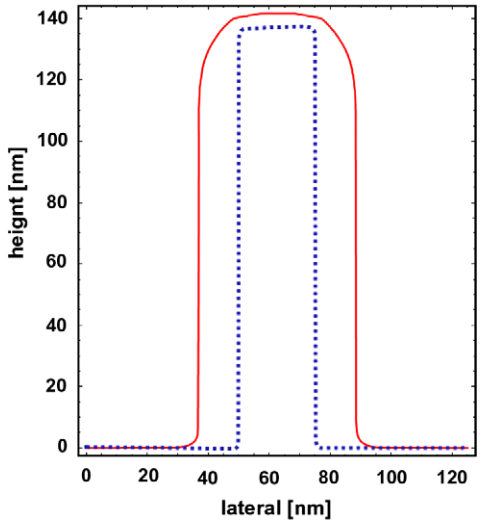

Fig. 5. Deposition of a pillar using a local model (dotted line) and a model considering the recoil range (solid line).

point is partly blocked by the surface. The improved model described at the end of Section 2.1 reduces this peak, although some deviation from the binary collision results remain.

Finally, Fig. 5 shows IonShaper® results of ion beam induced deposition with a 25 nm broad 10 keV Ar beam. The dotted line corresponds to the local model while the solid line represents the nonlocal model including the recoil range. It can be seen that the finite size of the recoil cascade significantly increases the width of the deposited pillar. The effect is particularly pronounced since a relatively low density of recoils causes a substantial growth of the material in beam assisted deposition.

4. Conclusions

Our assessment of models used for topography simulation of ion beam processes for 10 keV Ar ions and Si targets lets us conclude the following:

(i) The cosine distribution is only a rough approximation of the angular distribution of sputtered atoms. In particular sputtering of deep trenches requires an accurate description of the distribution at large backwards angles. Similarly, specular reflection is only a poor approximation for the reflected ions. In both cases implementation of tables in the topography simulator should be worthwhile.
(ii) Sputtering by reflected ions can be an important effect as has been seen in Fig. 1. In contrast, sputtering by sputtered particle is likely to be negligible because of the low average energy of the sputtered atoms.
(iii) A local model of sputtering as implemented in all topography simulators today results in significant artifacts. A model based on the spatial distribution of sputtered atoms on planar surfaces has been proposed and is expected to improve results for small structures. A nonlocal model is even more important for ion beam assisted deposition.

We plan to extend this study to other energies and ion species, and to study the influence of the proposed models on surface shapes.

Acknowledgments

This work has been partly supported by the European commission through funding of the CHARPAN integrated project and the Austrian Promotion Agency, Austrian Nano Initiative Program, NILaustria project.

References

[1] R.M. Langford, P.M. Nellen, J. Gierak, Y. Fu, MRS Bull. 32 (2007) 417.
[2] I. Utke, P. Hoffmann, J. Melngailis, J. Vac. Sci. Technol. B26 (2008) 1197.
[3] E. Platzgummer, H. Loeschner, G. Gross, Proc. SPIE Vol. 6730 (2007).
[4] E. Platzgummer, H. Loeschner, G. Gross, J. Vac. Sci. Technol. B, 2008.
[5] CHARPAN, <http://www.charpan.com/>.
[6] NILaustria, <http://www.nilaustria.at/>.
[7] A.R. Neureuther, C.Y. Liu, C.H. Ting, J. Vac. Sci. Technol. 16 (1979) 1767.
[8] N. Yamauchi, T. Yachi, T. Wada, J. Vac. Sci. Technol. A2 (1984) 1552.
[9] H. Ximen, R.K. DeFreez, J. Orloff, R.A. Elliot, G.A. Evans, N.W. Carlson, W. Carlson, M. Lurie, D.P. Pour, J. Vac. Sci. Technol. B8 (1990) 1361.
[10] T. Ishitani, T. Ohnishi, J. Vac. Sci. Technol. A9 (1991) 3084.
[11] I.V. Katardjiev, G. Carter, M.J. Nobes, S. Berg, H.O. Blom, J. Vac. Sci. Technol. A12 (1994) 61.
[12] M.J. Vasile, J. Xie, R. Nassar, J. Vac. Sci. Technol. B17 (1999) 1085.
[13] D.P. Adams, M.J. Vasile, J. Vac. Sci. Technol. B24 (2006) 836.
[14] E. Platzgummer, A. Biedermann, H. Langfischer, S. Eder-Kapl, M. Kuemmel, S. Cernusca, H. Loeschner, C. Lehrer, L. Frey, A. Lugstein, E. Bertagnolli, Microelectron. Eng. 83 (2006) 936.
[15] H.-B. Kim, G. Hobler, A. Lugstein, E. Bertagnolli, J. Micromech. Microeng. 17 (2007) 1178.
[16] H.-B. Kim, G. Hobler, A. Steiger, A. Lugstein, E. Bertagnolli, Nanotechnology 18 (2007) 245303.
[17] Y. Yamamura, T. Takiguchi, H. Tawara, Rep. NIFS-DATA-1, Nat. Inst. Fusion Sci., Nagoya, Japan, 1990.
[18] J.S. Ro, C.V. Thompson, J. Melngailis, J. Vac. Sci. Technol. B12 (1994) 73.
[19] G. Hobler, Nucl. Instr. and Meth. B96 (1995) 155.
[20] W. Eckstein, Computer Simulation of Ion–Solid Interactions, Springer, 1991.
[21] P.C. Zalm, J. Appl. Phys. 54 (1983) 2660.
[22] Y. Yamamura, H. Tawara, Rep. NIFS-DATA-23, Nat. Inst. Fusion Sci., Nagoya, Japan, 1995.